TRANSACTIONS ON ELECTRICAL AND ELECTRONIC MATERIALS
Vol. 15, No. 3, pp. 164-169, June 25, 2014

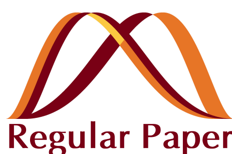


pISSN: 1229-7607 eISSN: 2092-7592
DOI: http://dx.doi.org/10.4313/TEEM.2014.15.3.164

# Dry Etching Properties of $HfAlO_3$ Thin Film with Addition $O_2$ gas Using a High Density Plasma

Jong-Chang Woo†
*Nano Convergence Sensor Research Section, Electronics and Telecommunications Research Institute, Daejeon 305-700, Korea*

Yong-Bong Lee
*Convergence Components & Materials Research Laboratory, Electronics and Telecommunications Research Institute, Daejeon 305-700, Korea*

Jeong-Ho Kim
*Department of Computer Engineering, Hanbat National University, Daejeon 305-719, Korea*

**Received February 7, 2014; Revised May 1, 2014; Accepted May 19, 2014**

We investigated the etching characteristics of $HfAlO_3$ thin films in $O_2/Cl_2/Ar$ and $O_2/BCl_3/Ar$ gas, using a high-density plasma (HDP) system. The etch rates of the $HfAlO_3$ thin film obtained were 30.1 nm/min and 36 nm/min in the $O_2/Cl_2/Ar$ (3:4:16 sccm) and $O_2/BCl_3/Ar$ (3:4:16 sccm) gas mixtures, respectively. At the same time, the etch rate was measured as a function of the etching parameter, namely as the process pressure. The chemical states on the surface of the etched $HfAlO_3$ thin films were investigated by X-ray photoelectron spectroscopy. Auger electron spectroscopy was used for elemental analysis on the surface of the etched $HfAlO_3$ thin films. These surface analyses confirm that the surface of the etched $HfAlO_3$ thin film is formed with nonvolatile by-product. Also, Cl-O can protect the sidewall due to additional $O_2$.

**Keywords:** Etch, XPS, AES, $HfAlO_3$, ICP

## 1. INTRODUCTION

Recently, the scaling down of $SiO_2$ thickness has exacerbated problems such as increased leakage current, poly-Si gate depletion, and boron penetration into the channel region. Therefore, the still high-*k* materials, such as $HfO_2$, $Al_2O_3$, and $HfAlO_3$, have been studied as substitutes for $SiO_2$, as the insulator layer of transistors [1-6]. These high-*k* films can be used as insulators for metal-insulator-metal (MIM) capacitors, to improve the packing density of integrated circuits, by increasing the dielectric constant of the insulators [7-9]. However, new insulator candidates must satisfy the CMOS processing procedure. In addition, it is very important to use $HfAlO_3$ as the insulator, in order to achieve a high etch rate and good profile, for the sake of the throughput and reliability of the MIM capacitor.

In this work, we investigated the etch characteristics of the $HfAlO_3$ thin films, using an inductively coupled plasma (ICP) system. The etching characteristics of the $HfAlO_3$ thin film were investigated in terms of the selectivity of $HfAlO_3$ to $SiO_2$ as a function of added $O_2$ gas in Cl-based gas chemistry. The chemical states on the surface of the etched $HfAlO_3$ thin film were investigated by X-ray photoelectron spectroscopy (XPS). Auger electron spectroscopy (AES) was used for elemental analysis on the surfaces of the etched $HfAlO_3$ thin film. Field emission-scanning electron microscopy (FE-SEM) was used to investigate the etch profile.

† Author to whom all correspondence should be addressed:
E-mail: wjch97@etri.re.kr

Copyright ©2014 KIEEME. All rights reserved.
This is an open-access article distributed under the terms of the Creative Commons Attribution Non-Commercial License (http://creativecommons.org/licenses/by-nc/3.0) which permits unrestricted noncommercial use, distribution, and reproduction in any medium, provided the original work is properly cited.

## 2. EXPERIMENTAL

The $HfAlO_3$ thin films were deposited on $SiO_2$/Si 6-in p-type (100) wafers, by an atomic layer deposition (ALD) system. $HfAlO_3$ thin film was deposited on the $SiO_2$(100 nm)/Si(100) by ALD, with a thickness of 200 nm. The dry etching of the $HfAlO_3$ thin films was performed, using an ICP system [10,11]. A 13.56 MHz power generator was connected to a 3.5 turn copper coil, to generate the ICP. Another 13.56 MHz power generator was attached to the substrate electrode, to control the DC-bias voltage. The substrate temperature was kept at 30℃, with a water-cooling system. The chamber was pumped to $10^{-4}$ Pa. The final pressure was lower than $10^{-4}$ Pa, using a turbo-molecular pump. The etching characteristics of the $HfAlO_3$ thin films were investigated as functions of the $O_2/Cl_2/Ar$ and the $O_2/BCl_3/Ar$ gas mixing ratio. The etching conditions of the RF power, DC-bias voltage, and process pressure were 600 W, - 150 V, and 1 Pa, respectively. The etch rates were measured, using a surface profiler (Alpha-Step 500, KLA-Tencor). AES analyses were performed with a scanning auger microprobe (Microlab 350, VG Scientific). The composition change on the surface of the etched $HfAlO_3$ thin film was analyzed by XPS. The XPS spectra were collected using a VG Scientific ESCALAB 250 instrument, equipped with an analytical chamber. The chamber was pumped down to a base pressure of less than $10^{-8}$ Pa with a twin-anode x-ray source, and a spherical sector analyzer with multichannel detectors. The samples were mounted on stainless steel stubs using double-sided adhesive tape, and Al *Kα* radiation ($h\nu$ = 1,486.6 eV) was used as an X-ray source. All XPS data were corrected for sample charging during x-ray irradiation, using the adventitious hydrocarbon referencing peak (C 1s at 284.6 eV). The etching profile of the cross-section was characterized using FE-SEM (Sirion 400, FEI). The $HfAlO_3$ thin films used for measuring the etch rate and etching profile had a PR pattern, with width and thickness of 1.63 ㎛ both.

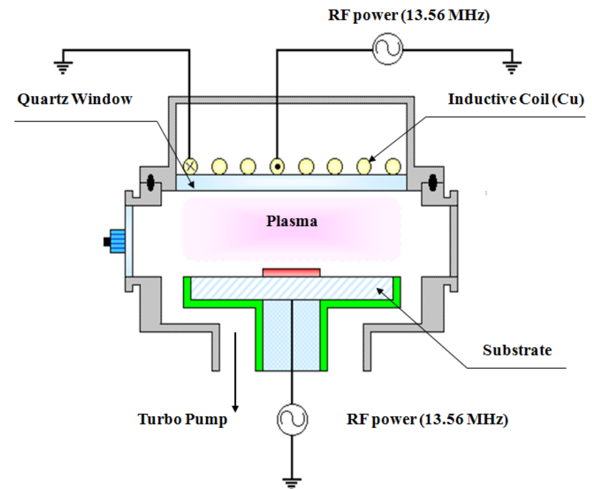


Fig. 1. Inductively coupled plasma system.

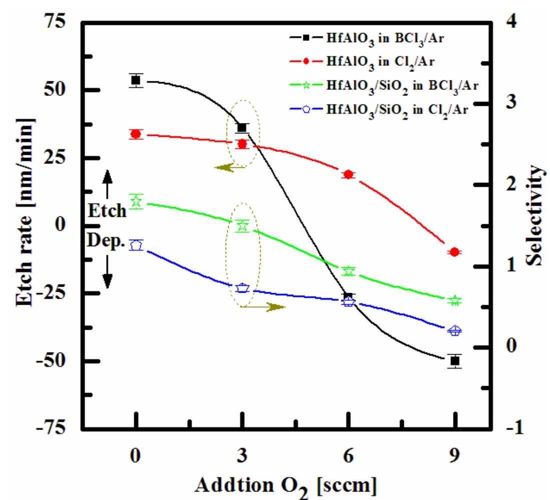


Fig. 2. Etch rate of $HfAlO_3$ thin films and the selectivity of $HfAlO_3$ to $SiO_2$, as a function of the $O_2/BCl_3/Ar$ and $O_2/Cl_2/Ar$ gas mixing ratios.

## 3. RESULTS AND DISCUSSION

### 3.1 The effect of added $O_2$ gas in the $BCl_3$- and $Cl_2$-based gas mixture

To evaluate the etch characteristics of the $HfAlO_3$ thin films in an ICP etching system, the $HfAlO_3$ thin films were etched by varying the $BCl_3/Ar$ and $Cl_2/Ar$ gas chemistry. The etch characteristics of the film in chlorine plasma need to be studied, when chlorine gas was used for the $HfAlO_3$ thin film etching process. So, we investigated the etching characteristics of $HfAlO_3$ thin film in $BCl_3$- and $Cl_2$- inductively coupled plasma. The $O_2$ gas was added for passivation of the etching profile and the etch rate in the $BCl_3/Ar$ and $Cl_2/Ar$ mixing ratio [11]. Figure 2 shows the etch rate of $HfAlO_3$ thin film, and the selectivity of $HfAlO_3$ to $SiO_2$ as a function of $O_2$ content in the $Cl_2/Ar$ and $BCl_3/Ar$ gas mixture. The other conditions, of the RF power, DC-bias voltage, and process pressure, were kept at 600 W, - 150 V, and 1 Pa, respectively. The etch rate of the $HfAlO_3$ thin film and the selectivity of the $HfAlO_3$ to $SiO_2$ were 36 nm/min and 1.5, and 30.1 nm/min and 0.73, in the $O_2/BCl_3/Ar$(=3:4:16) and $O_2/Cl_2/Ar$(=3:4:16) gas mixtures, respectively. As the $O_2$ concentration increased from 0 to 9 sccm in the $BCl_3/Ar$ (=4:16) gas mixture, the etch rate of the $HfAlO_3$ thin films and the selectivity of $HfAlO_3$ to $SiO_2$ decreased from 53.54 to -50.05 nm/min, respectively. As the $O_2$ concentration increased from 0 to 9 sccm in the $Cl_2/Ar$ (=4:16) gas mixture, the etch rate of the $HfAlO_3$ thin film decreased from 33.7 to -9.8 nm/min. In our opinion, the domination of the chemical reactions can be explained by the following factors. A) The melting points of $HfCl_4$ and $AlCl_3$ are about 432 and 192.6℃, and the domination of the chemical pathway may be related to its lack of volatility; by contrast, the melting points of the Hf-$Cl_4$ and Al-$Cl_3$ are lower than the melting point of Hf-Al-O (=up to 2,000℃). B) The Hf-Cl and Al-Cl chemical bonds (kJ/mol) have a lower Gibb's free energy. The decrease of chemical bonds was due to the decreasing density of BCl or Cl radicals by reaction with O radicals, because the BCl and Cl atoms formed in the plasma spontaneously reacted with $HfAlO_3$ [12,13].

Figure 3 shows the etch rate of $HfAlO_3$ thin film as a function of the process pressure, in the $O_2/BCl_3/Ar$(=3:4:16 sccm) plasma. As the process pressures increased from 0.5 to 2.0 Pa, the etch rates of $HfAlO_3$ thin film decreased from 45.9 to 23.74 nm/min. The decrease of the process pressure enhances the density of the chemically neutral active species, which accelerates the chemical reaction [23]. However, since the mean free path and energy of the ions decrease with decreasing process pressure, the ion stimulated desorption of the reaction products is decreased, and the fraction of free surface available for the chemical reaction is increased. As a result of the pressure effect on the etch rate of the $HfAlO_3$ thin film, the etch process is limited by the supply of the chemical source; and thus, the etch rate of $HfAlO_3$ thin film decreases with decreasing process pressure [16].

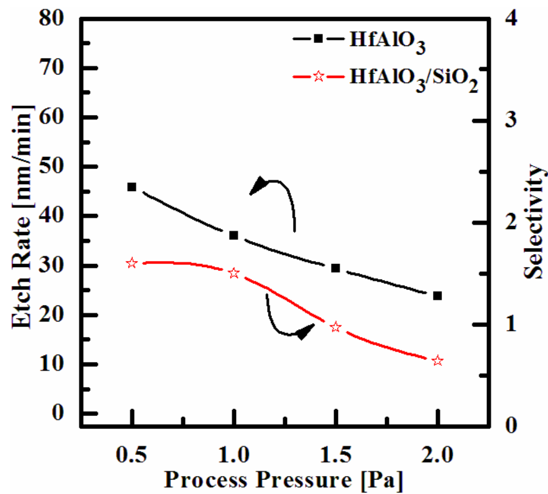


Fig. 3. Etch rate of $HfAlO_3$ thin films and the selectivity of $HfAlO_3$ to $SiO_2$, as a function of the process pressure.

## 3.2 Surface analysis

The samples were investigated by XPS and AES, to analyze the chemical states on the surface of the etched $HfAlO_3$ thin films exposed to the $O_2/Cl_2/Ar$(=3:4:16 sccm) and $O_2/BCl_3/Ar$(=3:4:16 sccm) plasmas. The input plasma parameters were set to an RF power of 600 W, DC-bias voltage of - 150 V, process pressure of 1 Pa, and substrate temperature of 30℃. No boron peaks were detected. This means that the boron and chlorine compounds are highly volatile ones, such as boron-oxy-chloride (BOCl) or trichloro-boroxin $(BOCl)_3$ [24].

Figure 4 shows the AES surface scan spectra of the $HfAlO_3$ thin film for (a) the as-deposited films and the surface of the etched $HfAlO_3$ thin films in (b) the $O_2/Cl_2/Ar$, and (c) $O_2/BCl_3/Ar$ plasma, respectively. The etching time of the $HfAlO_3$ thin film was 10 sec. Figure 4 (a) shows an AES surface scan of the as-deposited $HfAlO_3$ thin film, in which O peaks are detected. The origin of carbon elements is the contamination in the etching chamber or the air. After etching, no B or Cl-related peaks were observed. With the addition of $O_2$ gas, the intensity of Hf, Al and O peaks decreased, compared to that of the etched sample in $BCl_3/Ar$ and $Cl_2/Ar$ plasmas. This result means that by-products, such as $Hf\text{-}O_x$ and $Al_x\text{-}O_y$, increased on the etched surface in $O_2/BCl_3/Ar$ and $O_2/Cl_2/Ar$ plasmas. Therefore, the AES data clearly show that the surface of the etched $HfAlO_3$ thin films in $O_2/BCl_3/Ar$ and $O_2/Cl_2/Ar$ plasmas are formed with nonvolatile etch products, such as $Hf\text{-}O_x$, $Al_x\text{-}O_y$, $Hf\text{-}Cl_x$, and $Al\text{-}Cl_x$ .

Figure 5 shows the deconvoluted peaks of the Hf 4f XPS narrow scan spectra for (a) the as-deposited films and the surface of the etched $HfAlO_3$ thin films in (b) the $O_2/Cl_2/Ar$, and (c) $O_2/BCl_3/Ar$ plasma, respectively. Figure 4(a) shows the Hf 4f peak from the as-deposited $HfAlO_3$ thin film, which must originate from Hf-O or Hf-Al-O bonds. It can be seen that the Hf 4f peak can be deconvoluted into two peaks, viz. Hf-O or Hf-Al-O (18.7, 17.1 eV). As shown in Figs. 5(b) and (c), it can be seen that when the $HfAlO_3$ thin films were exposed to both the $O_2/Cl_2/Ar$ (3:4:16 sccm) plasma and $O_2/BCl_3/Ar$ (3:4:16 sccm) plasma, new peaks of Hf-Cl bonds appear at 17.2 eV and 16.5 eV (in $O_2/Cl_2/Ar$ plasma), and 18.2 eV and 16.5 eV (in $O_2/BCl_3/Ar$ plasma), which were higher binding energy by about ±0.1 eV. When adding $O_2$ to $Cl_2/Ar$ plasma and $BCl_3/Ar$ plasma, the intensity of Hf-O or Hf-Al-O, and Hf-Cl bonds decreased, but the intensity of Hf-O or Hf-Al-O bonds $O_2/BCl_3/Ar$ plasma is higher than in $O_2/Cl_2/Ar$ plasma [22]. This result means that

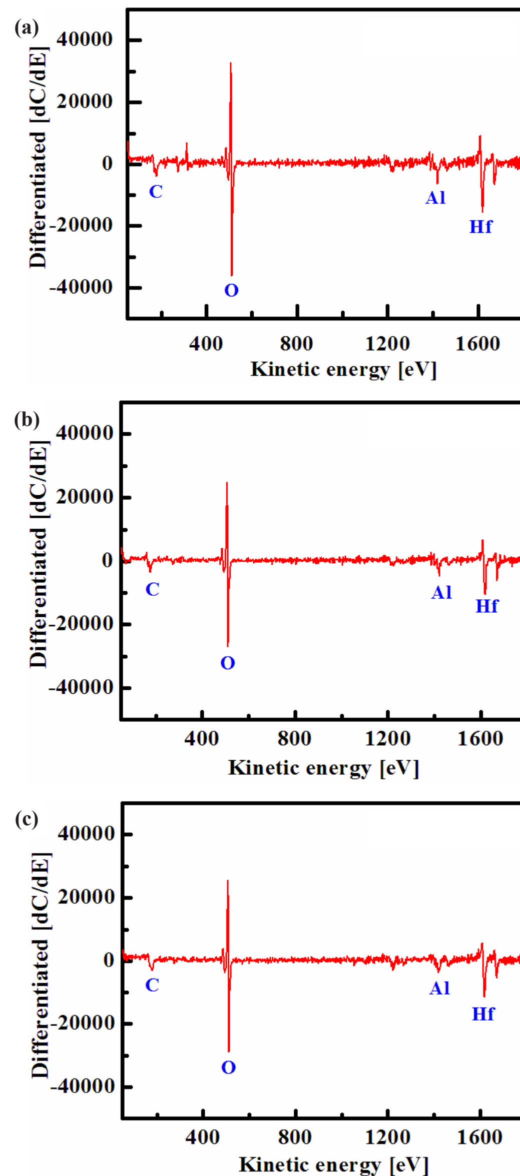


Fig. 4. AES surface scan of the etched $HfAlO_3$ thin films, as a function of etch chemistry. (a) As-deposited, (b) $O_2/Cl_2/Ar$, and (c) $O_2/BCl_3/Ar$.

by-products, such as $Hf\text{-}O_x$ and $Al_x\text{-}O_y$, in $O_2/BCl_3/Ar$ plasma increased on the etched surface, rather than in the $O_2/Cl_2/Ar$ plasma. The XPS data give clear confirmation that etching of the $HfAlO_3$ thin film in the $O_2/Cl_2/Ar$ and $O_2/BCl_3/Ar$ plasmas results in the formation of $Hf\text{-}Cl_x$ bonds on its surface. Thus, the etch rate of $HfAlO_3$ thin films increased, at the $O_2$ flow rate of 3 sccm [17,18]

Figure 6 shows the Al 2p peaks of the XPS narrow scan spectra of the as-deposited and the etched $HfAlO_3$ thin films in the $O_2/Cl_2/Ar$ and $O_2/BCl_3/Ar$ plasmas. The Al 2p peaks were not deconvoluted, because their intensity was too low. The Al 2p peaks of binding energy were not shifted, but the intensity of increased peaks in $O_2/BCl_3/Ar$ and in $O_2/Cl_2/Ar$ plasma is higher, than in as-deposited film. This result means that the Al atoms of the $HfAlO_3$ react with the Cl and O radicals. We supposed that the fluorine compounds, such as $Al\text{-}Cl_x$, remained on the surface of the $HfAlO_3$ thin film.

Figure 7 shows the deconvoluted peaks of the O 1s XPS narrow scan spectra for (a) the as-deposited films and the surface of the etched $HfAlO_3$ thin films, in (b) the $O_2/Cl_2/Ar$, and (c) the

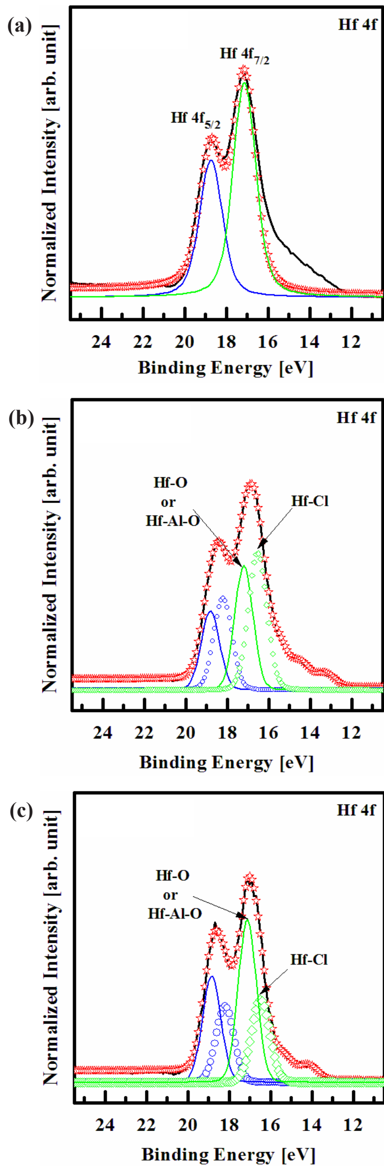


Fig. 5. Hf 4f XPS narrow spectra on the surface, as a function of the etch chemistry. (a) As-deposited, (b) $O_2/Cl_2/Ar$, and (c) $O_2/BCl_3/Ar$.

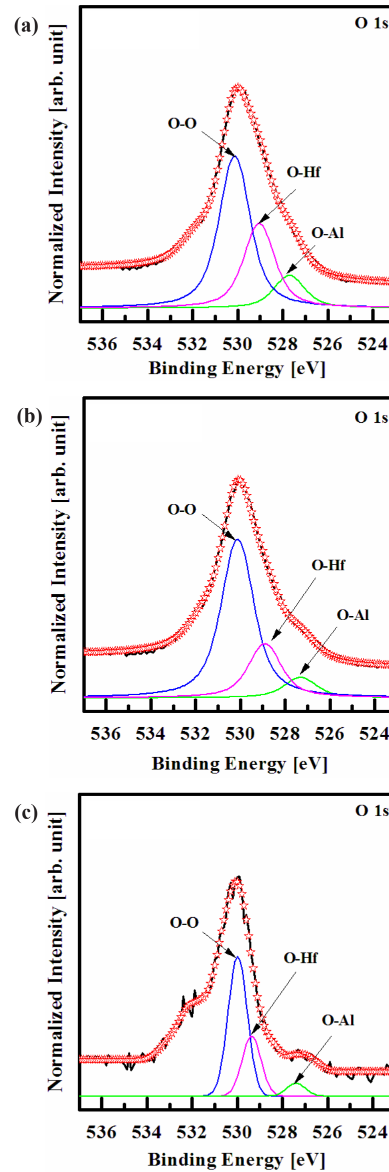


Fig. 7. O 1s XPS narrow spectra on the surface, as a function of the etch chemistry. (a) As-deposited, (b) $O_2/Cl_2/Ar$, and (c) $O_2/BCl_3/Ar$.

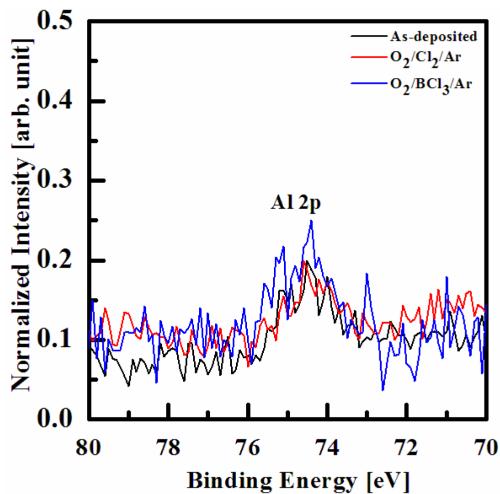


Fig. 6. Al 2p XPS narrow spectra on the surface, as a function of the etch chemistry.

$O_2/BCl_3/Ar$ plasmas, respectively. For the O 1s peak, the peaks at 530.1, 529, and 527.7 eV correspond to those of O-O, O-Hf, and O-Al, which originate from the interface of $HfAlO_3$ thin film. As shown in Figs. 7(b) and (c), the shoulder peaks of O-O, O-Hf, and O-Al decreased significantly in the $O_2/Cl_2/Ar$ and the $O_2/BCl_3/Ar$ plasmas, as a result of the preferential removal of Hf, Al, and O. However, when the $HfAlO_3$ thin films were etched in the $O_2/Cl_2/Ar$ and the $O_2/BCl_3/Ar$ plasmas, the O 1s peak intensity at 530.1, 529, and 527.7 eV decreased, due to the formation of Cl-O bonds [20]. The intensity of the O 1s peak for the surface of the etched $HfAlO_3$ thin film in $O_2/BCl_3/Ar$ plasma was higher than that of the etched $HfAlO_3$ thin film in the $O_2/Cl_2/Ar$ plasma. This is due to the dramatic increase in the number of Cl-O bonds, resulting from the effective dissociation of the Hf-Al-O bonds by ion bombardment. Based on the XPS result, it was revealed that Hf, Al, and O were removed by the chemical reactions with the Cl radicals, and the physical bombardment of the Ar ions [20-22].

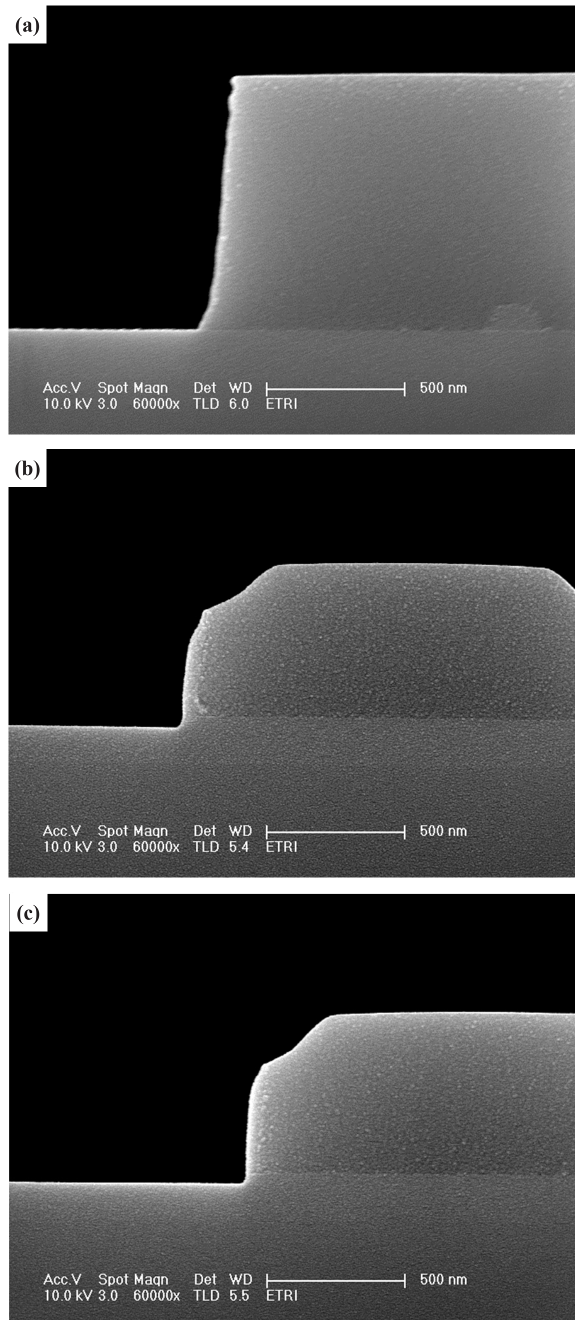


Fig. 8. Cross-sectional SEM image of the $HfAlO_3$ thin film. (a) As-deposited, (b) $O_2/Cl_2/Ar$ plasma, and (c) $O_2/BCl_3/Ar$ plasma.

### 3.3 FE-SEM analysis

Figure 8 shows cross-sectional SEM images of the $HfAlO_3$ thin film for (a) the as-deposited films and the surface of the etched $HfAlO_3$ thin films, in (b) the $O_2/BCl_3/Ar$ plasmas, at a process pressure of 1 Pa, RF power of 600 W, DC-bias voltage of - 150 V, and substrate temperature of 30℃. As shown in Figs. 8(b) and (c), a clean surface and side wall on the PR and $HfAlO_3$ thin film were obtained with the PR mask erosion. It may be possible, in order to obtain a high etch rate and a vertical etching profile, to also change the etching conditions to be higher than the existing experimental. So, PR mask erosion was caused by the physical etch pathway. But, the experimental results showed that the vertical etching profile of the $HfAlO_3$ thin film was obtained by the RIE using Cl radicals, due to the high etch rate of the $HfAlO_3$ thin film.

## 4. CONCLUSIONS

The etching characteristics of the $HfAlO_3$ thin film were investigated in the $O_2/Cl_2/Ar$ and the $O_2/BCl_3/Ar$ plasmas. The etch rate of the $HfAlO_3$ thin film were 30.1 nm/min, 36 nm/min in the $O_2/Cl_2/Ar$(=3:4:16 sccm) and the $O_2/BCl_3/Ar$(=3:4:16) gas mixture. As the $O_2$ fraction in the $Cl_2/Ar$ and $BCl_3/Ar$ plasmas was increased from 0 to 9 sccm, the etch rate of $HfAlO_3$ thin film decreased. In order to the $O_2/BCl_3/Ar$(=3:4:16) gas mixture, the etch rate of the $HfAlO_3$ thin film in the $O_2/BCl_3/Ar$ plasma was higher, than in $O_2/Cl_2/Ar$ plasma. Also, passivation layer formation occurred on sidewall, because of the small amount of $O_2$. However, the etch rate of the $HfAlO_3$ thin film increased, with the further addition of $O_2$ gas. XPS was used to investigate the chemical states of the etched $HfAlO_3$ thin films. The etching mechanism of the $HfAlO_3$ thin film can be explained as follows: Ta interacted with the Cl radicals in the $BCl_3$- and $Cl_2$ - containing plasmas, but remained at the surface, due to the low volatility of Hf-$Cl_x$ and $Al_x$-$Cl_y$, which could be effectively removed with the help of ion bombardment.

## REFERENCES

[1] M. H. Shin, M. S. Park. N. E. Lee, J. Y. Kim, C. Y. Kim, and J. H. Ahn, *J. Vac. Sci. Technol. A*, **24**, 1373 (2006) [DOI: http://dx.doi.org/10.1116/1.2210944].

[2] B. Cheng, M. Cao, P. V. Vande, W. Greene, H. Stork, Z. Yu, and J. C. S. Woo, *IEEE Trans. Electron Devices*, **46**, 261 (1999) [DOI: http://dx.doi.org/10.1109/16.737469].

[3] J. Torfifard and A. K. B. A'ain, *ETRI Journal*, **35**, 226 (2013) [DOI: http://dx.doi.org/10.4218/etrij.13.0112.0300].

[4] Y. Ma, Y. Ono, L. Stecker, D. R. Evans, and S. T. Hsu, *IEDM Tech. Dig.*, 149 (1999).

[5] N. S. Ryu, J. H. Jung, and Y. C. Jeong, ETRI Journal, **34**, 885 (2012) [DOI: http://dx.doi.org/10.4218/etrij.12.1812.0024].

[6] J. Chen, W. J. Yoo, Z. Y. Tan, Y. Wang, and D. S. H. Chan, *J. Vac. Sci. Technol. A*, **22**, 1552 (2004) [DOI: http://dx.doi.org/10.1116/1.1705590].

[7] K. H. Doo, B. I. Y. Yoon, B. C. Lee, S. S. Lee, M. S. Han, and W. W. Kim, *ETRI Journal*, **34**, 827 (2012) [DOI: http://dx.doi.org/10.4218/etrij.12.1812.0046].

[8] Q. Li, K. M. Koo, W. M. Lau, P. F. Lee, J. Y. Dai, Z. F. Hou, and X. G. Gong, *Appl. Phys. Lett.*, **88**, 182903 (2006) [DOI: http://dx.doi.org/10.1063/1.2196470].

[9] R. M. Martin, H. O. Blom, and J. P. Chang, *J. Vac. Sci. Technol. A*, **27**, 217 (2009) [DOI: http://dx.doi.org/10.1116/1.3065695].

[10] J. C. Woo, T. K. Ha, D. S. Um, J. Y. Park, Y. C. Kang, and C. I. Kim, *Thin Solid Films*, **520**, 1141 (2011) [DOI: http://dx.doi.org/10.1016/j.tsf.2011.08.078].

[11] T. K. Ha, J. C. Woo, and C. I. Kim, *Vacuum*, **85**, 932 (2011) [DOI: http://dx.doi.org/10.1016/j.vacuum.2011.01.015].

[12] W. S. Hwang, J. Chen, W. J. Yoo, and V. Bliznetsov, *J. Vac. Sci. Technol. A*, **23**, 964 (2005) [DOI: http://dx.doi.org/10.1116/1.1927536].

[13] J. Tonotani, T. Iwamoto, F. Sato, K. Hattori, S. Ohmi, and H. Iwai, *J. Vac. Sci. Technol. B*, **21**, 2163 (2003) [DOI: http://dx.doi.org/10.1116/1.1612517].

[14] J. I. Won, J. G. Koo, T. P. Rhee, H. S. Oh, and J. H. Lee, *ETRI Journal*, **35**, 603 (2013) [DOI: http://dx.doi.org/10.4218/etrij.13.1912.0030].

[15] H. J. Lee, B. S. Kwon, H. W. Kim, S. I. Kim, D. G. Yoo, J. H. Boo,

and N. E. Lee, *Jpn. J. Appl. Phys.*, **47**, 6960 (2008) [DOI: http://dx.doi.org/10.1143/JJAP.47.6960].

[16] M. H. Shin, S. W. Na, N. E. Lee, T. K. Oh, J. Kim, T. Lee, and J. Ahn, Jpn. J. Appl. Phys., 44, 5811 (2005) [DOI: http://dx.doi.org/10.1143/JJAP.44.5811].

[17] E. Jud, M. Tang, and Y. M. Chiang, J. Appl. Phys., 103, 114108 (2008) [DOI: http://dx.doi.org/10.1063/1.2937900

[18] H. Jin, U. K. Oh, H. J. Kang, S. W. Lee, Y. S. Lee, and K. Y. Lim, *J. Korean Phys. Soc.*, **46**, S52 (2005).

[19] R. Tan, Y. Azuma, and I. Kojima, *Appl. Surf. Sci.*, **241**, 135 (2005) [DOI: http://dx.doi.org/10.1016/j.apsusc.2004.09.030].

[20] L. P. Feng, Z. T. Liu, and Y. M. Shen, *Vacuum*, **83**, 902 (2009) [DOI: http://dx.doi.org/10.1016/j.vacuum.2008.08.004].

[21] L. Zhang, S. Y. Terauchi, Y. Azuma, and T. Fujimoto, *Surf. Interface Anal.*, **40**, 1701 (2008) [DOI: http://dx.doi.org/10.1002/sia.2901].

[22] X. Cheng, L. Wan, Z. Song, Y. Yu, and D. Shen, *Appl. Phys. Lett.*, **90**, 152910 (2007) [DOI: http://dx.doi.org/10.1063/1.2722665].

[23] H. K. Chiu, T. L. Lin, Y. Hu, K. C. Leou, H. C. Lin, M. S. Tsai, and T. Y. Huang, *J. Vac. Sci. Technol. A*, **19**, 455 (2001) [DOI: http://dx.doi.org/10.1116/1.1342866].

[24] A. M. Efremov, D. P. Kim, and C. I. Kim, *J. Vac. Sci. Technol. B*, **75**, 133 (2004).